metals

MDPI

Article

Evolution of the Microstructure and Mechanical Properties of AZ31 Magnesium Alloy Sheets during Multi-Pass Lowered-Temperature Rolling

Qing Miao [1], Lantao Zhu [2], Wenke Wang [2,*], Zhihao Wang [3], Bin Shao [4], Wenzhen Chen [2], Yang Yu [2] and Wencong Zhang [2]

[1] School of Materials, Shanghai Dian Ji University, Shanghai 201306, China
[2] School of Materials Science and Engineering, Harbin Institute of Technology, Weihai 264209, China
[3] Laboratoire de Génie Civil et Génie Mécanique—EA 3913, INSA Rennes, University Rennes, F-35000 Rennes, France
[4] National Key Laboratory for Precision Hot Pressing of Metals, Harbin Institute of Technology, Harbin 150001, China
* Correspondence: 15b309020@hit.edu.cn; Tel.: +86-631-567-2167; Fax: +86-631-567-2167

Abstract: AZ31 magnesium alloy sheets with 2 mm thickness were successfully fabricated by multi-pass lowered-temperature rolling. The evolution of the microstructure, texture, and mechanical properties during the rolling process was investigated. Based on the effect of multiple dynamic recrystallization, multi-pass lowered-temperature rolling not only refined the grain size obviously but also markedly improved the microstructure homogeneity. The resulting sheets had the optimal microstructure morphology with an average grain size of 4.38 μm. For the texture evolution, the stress state of the rolling process made the (0002) basal plane gradually rotate toward the rolling plane. However, the activation of non-basal slips due to the higher rolling temperature slightly rotated the (0002) basal plane point to the rolling direction (RD). As a result, the grain refinement strengthening and the texture strengthening together increased the yield stress to 202 MPa in the transverse direction (TD) and 189.8 MPa in the RD. Importantly, the resulting sheet concurrently exhibited excellent fracture elongation, about 38% in the TD and 39.2% in the RD. This was mainly ascribed to the finer grain size, giving rise to a significant effect of grain boundary sliding and the activation amount of non-basal slips.

Keywords: magnesium alloy; dynamic recrystallization; grain size; texture; elongation

Citation: Miao, Q.; Zhu, L.; Wang, W.; Wang, Z.; Shao, B.; Chen, W.; Yu, Y.; Zhang, W. Evolution of the Microstructure and Mechanical Properties of AZ31 Magnesium Alloy Sheets during Multi-Pass Lowered-Temperature Rolling. *Metals* **2022**, *12*, 1811. https://doi.org/10.3390/met12111811

Academic Editor: Talal Al-Samman

Received: 27 September 2022
Accepted: 18 October 2022
Published: 26 October 2022

1. Introduction

Magnesium alloys are considered to be the lightest structural metallic alloys, resulting in marked increases in their use in automobile parts and electric appliance cases [1–3]. In magnesium alloy products, magnesium alloy sheets have a very large market demand. However, the hexagonal close-packed (HCP) structure in magnesium alloys only activates two independent basal slips at room temperature [4]. This results in their poor formability, which is an important factor restricting their wide use in critical safety components [5]. In order to meet the demand, it is necessary to develop rolling technologies for the mass production of magnesium alloy sheets with high performance (high strength and high formability simultaneously).

It is well known that grain refinement and texture weakening are factors that improve the formability of magnesium alloy sheets [6–8]. Huang et al. fabricated various AZ31 magnesium alloy sheets with a grain size from 7 μm to 16 μm and found that both stretch formability and deep drawability deteriorated with the increase in grain size [7]. They attributed the reason to the small grain size that restricted tension twin activity and finally delayed the texture strengthening [7]. In Huo's study, the tensile ductility and

stretch formability of AZ31 magnesium alloy sheets fabricated by cross-wavy bending were distinctly enhanced compared to the initial sheets (about 1.55 and 2 times, respectively) [9]. In their view, these prominent increases were mainly ascribed to the fine-grained microstructure with an average grain size of 8 μm and a weak and random basal texture [9]. Currently, abundant plastic process techniques can refine the grain size and tailor the basal texture synchronously, for example, multi-pass lowered-temperature rolling [10], twin-roll casting [11], different speed rolling [12], and equal channel angular rolling [13]. However, these techniques cannot realize grain refinement and texture weakening or the high efficiency of industrial sheet fabrication. In the above process methods, multi-pass lowered-temperature rolling is considered to be the most suitable method for industrial sheet fabrication due to the absence of intermediate annealing [10]. This is very important to the mass production of magnesium alloy sheets. Moreover, prior work verified that multi-pass lowered-temperature rolling could fabricate magnesium alloy sheets with high performance [14,15]. Such an effect might be ascribed to the occurrence of multiple dynamic recrystallization (DRX), which helped to refine the grain size and improve the microstructure homogeneity during the rolling process. Accordingly [16], the DRX grain size was closely related to the rolling process parameters, which can be well explained by the Zener–Hollomon Z ($Z = \dot{\varepsilon}\exp(\mathrm{Q}/\mathrm{R}T)$, where $\dot{\varepsilon}$ is the strain rate, T is the deformation temperature, Q is the activation energy, and R is the gas constant). Actually, the strategy of a lower temperature was designed during multi-pass rolling, which was because such a strategy can increase the recrystallization nucleation sites and inhibit the grain boundary migration. Therefore, multi-pass lowered-temperature rolling can significantly improve the microstructure of magnesium alloys. However, the present rolling technologies usually use thick magnesium alloy plates as the initial material, which need multiple rolling passes to realize the fabrication of thin sheets, i.e., only by reasonable matching of the rolling parameters under each rolling pass can the microstructure of the resulting sheets be improved as much as possible. This makes it necessary to investigate the evolution of the microstructure and mechanical properties during multi-pass hot rolling. For this purpose, this work investigated the multi-pass lowered-temperature rolling of as-cast AZ31 magnesium alloy sheets in order to fabricate thin sheets with better microstructure and high performance. The reason for the enhancement of elongation arising from grain refinement was mainly discussed.

2. Materials and Methods

The initial material in this work was the as-cast AZ31 magnesium alloy plates with 30 mm thickness. Their nominal composition was determined as Mg, 3 wt.%; Al, 1 wt.%; Zn, 0.2 wt.%; and Mn by an inductively coupled plasma analyzer (ICP, Thermo Corp., Waltham, MA, USA). These initial materials were homogenized at 400 °C for 24 h in an electric furnace to improve component segregation and eliminate possible intercrystalline phases according to the literature [17]. Moreover, in order to improve their workability, all sheets were preheated to 400 °C for 30 min prior to hot rolling. In this work, all thickness reductions were set to 20% at break-down rolling pass in order to avoid premature cracking and then increased to 30% to improve the degree of DRX. According to previous studies, a lower deformation temperature easily realizes grain refinement. Therefore, in order to refine the grain size effectively, the rolling temperature tended to decrease as the rolling proceeded, i.e., 400 °C (Pass 1), 380 °C (Pass 2), 360 °C (Pass 3), 340 °C (Pass 4), 320 °C (Pass 5), 300 °C (Pass 6), 280 °C (Pass 7), and 260 °C (Pass 8). The detailed rolling process parameters are summarized in Table 1.

Table 1. Rolling process parameters for AZ31 magnesium alloy.

Condition	Thickness Change, mm	Rolling Temperature, °C	Thickness Reduction, %
Pass 1	30 → 24	400	20
Pass 2	24 → 16.8	380	30
Pass 3	16.8 → 11.7	360	30
Pass 4	11.7 → 8.2	340	30
Pass 5	8.2 → 5.7	320	30
Pass 6	5.7 → 4	300	30
Pass 7	4 → 2.8	280	30
Pass 8	2.8 → 2	260	30

Microstructure characteristics were observed on the RD–TD plane (RD: rolling direction, TD: transverse direction) of the samples, which were machined from the sheets by wire-electrode cutting. These samples first experienced mechanical polishing and then chemical etching with a solution consisting of picric acid (5.5 g), acetic acid (2 mL), distilled water (10 mL), and ethanol (90 mL). Then, an OLYMPUS GX71 (Olympus Corp., Tokyo, Japan) optical microscope (OM) was applied for metallographic observations. In this work, the mean linear intercept method ($\overline{d_v} = 1.74\ \overline{L}$, $\overline{L}$ is the average linear intercept) was used to measure the average grain size. Regarding the texture measurement, the texture state of the initial material was characterized by X-ray diffraction (XRD) experiments and that of the as-rolled sheets by electron backscatter diffraction (EBSD). The preparation of EBSD samples consisted of soft diamond polishing and subsequent etching with electropolishing in a 5:3 solution of ethanol and phosphoric acid for 8 min at 0.25 A. Subsequently, these samples were measured by a JEOL 733 electron probe (JEOL Ltd., Tokyo, Japan) equipped with an HKL Channel 5 system. In this work, scanning electron microscopy (SEM) was used to identify the type of fracture of the tension samples. In addition, a TECNAL transmission electron microscopy (TEM, FEI Corp., Hillsboro, OR, USA) was used to characterize the microstructure details, and its accelerating voltage was 200 kV. Uniaxial tension tests were measured by an Instron 5569 machine (Instron Corp., Norwood, MA, USA) with a strain rate of $1 \times 10^{-3}\ s^{-1}$ at room temperature. The tension samples were cut along the rolling direction and the transverse direction and their gauges were 25 mm in length and 6 mm in width.

3. Results and discussion

3.1. Microstructure Characteristics

Figure 1 shows the microstructure of the initial material after homogenized annealing. Clearly, the initial material possessed a larger grain size of about 293.3 μm, but relatively speaking, the microstructure was homogeneous, demonstrating that the difference in grain size between RD and TD was small. The microstructure characteristics of as-rolled AZ31 magnesium alloy sheets during multi-pass lowered-temperature rolling are displayed in Figure 2, and their corresponding grain size distributions are summarized in Figure 3. Clearly, the microstructure in the Pass 1 sheet exhibited a combination of fine and coarse grains, but compared to the initial microstructure, significant grain refinement occurred, in which the average grain size decreased to 34.73 μm in the Pass 1 sheet (Figure 3a). In addition, abundant twins could be seen in coarse grains (Figure 2a). In the Pass 2 sheet, this microstructure feature (coarse grains containing twins) was still the dominant, but the coarse grains were surrounded by fine, equiaxed grains (Figure 2b). This revealed the DRX had occurred. Here, it is worth noting the reason for the activation of twinning in the initial stage of rolling. The coarse grain in the initial material was considered to be the major cause. More specifically, in coarse grains, the distance of the dislocation slip was longer, which generally led to severe dislocation pile-up and stress concentration at grain boundaries [18]. Therefore, such a stress concentration would promote the twinning activation. In addition, the crystal orientation was an important factor as well. The initial material in this work was the as-cast AZ31 magnesium alloy plates, and there were some

grains with the c-axes nearly perpendicular to the normal direction (ND) of the plate. Such crystal orientation was conducive to the activation of tension twinning when the compression force imposed on the plates occurred along the normal direction. However, as the rolling proceeded, abundant basal planes were rotated to the hard orientation. At this moment, the tension twinning lost its original advantage of crystal orientation and thereby was activated with difficulty. As a consequence, the coarse grain and the crystal orientation were two important reasons triggering the twinning activation, particularly at the initial stage of rolling. Importantly, for the magnesium alloys, the activation of twinning in the initial stage of rolling had two beneficial roles: (1) they could accommodate the rolling deformation and release stress concentration, avoiding premature cracking; (2) their twin boundaries could act as the preferred sites for DRX in the next rolling procedure, and this could be a softening mechanism to improve the workability, ensuring that subsequent rolling was done smoothly [18].

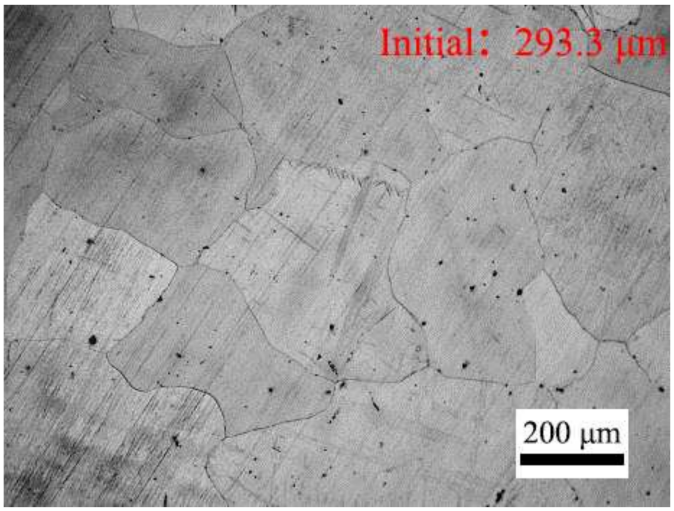

Figure 1. Metallographic observation of the initial material after homogenized annealing.

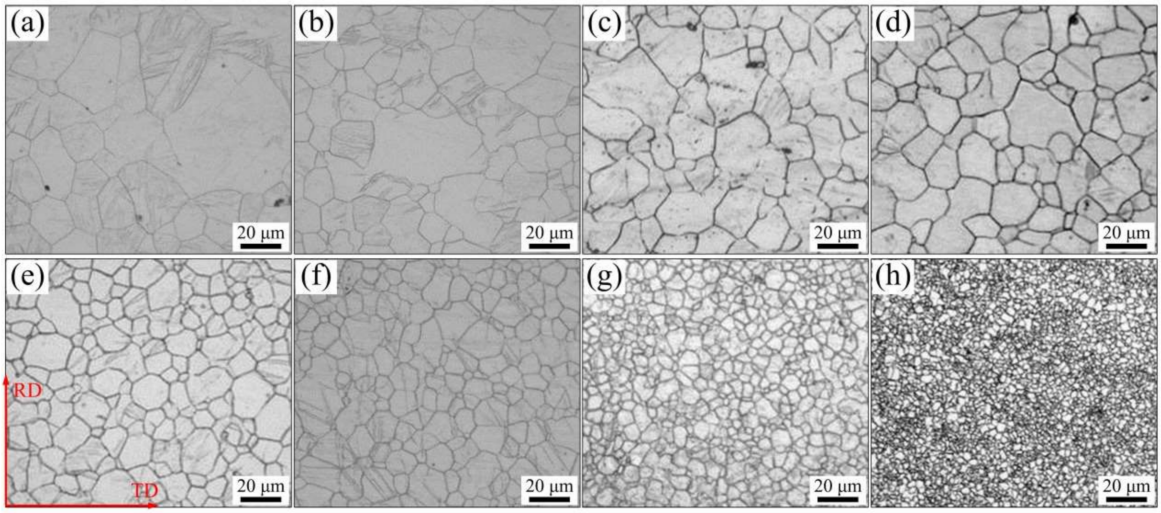

Figure 2. Microstructure characteristics of AZ31 magnesium alloy sheets during multi-pass lowered-temperature rolling: (**a**) Pass 1; (**b**) Pass 2; (**c**) Pass 3; (**d**) Pass 4; (**e**) Pass 5; (**f**) Pass 6; (**g**) Pass 7; (**h**) Pass 8. (RD: rolling direction, TD: transverse direction).

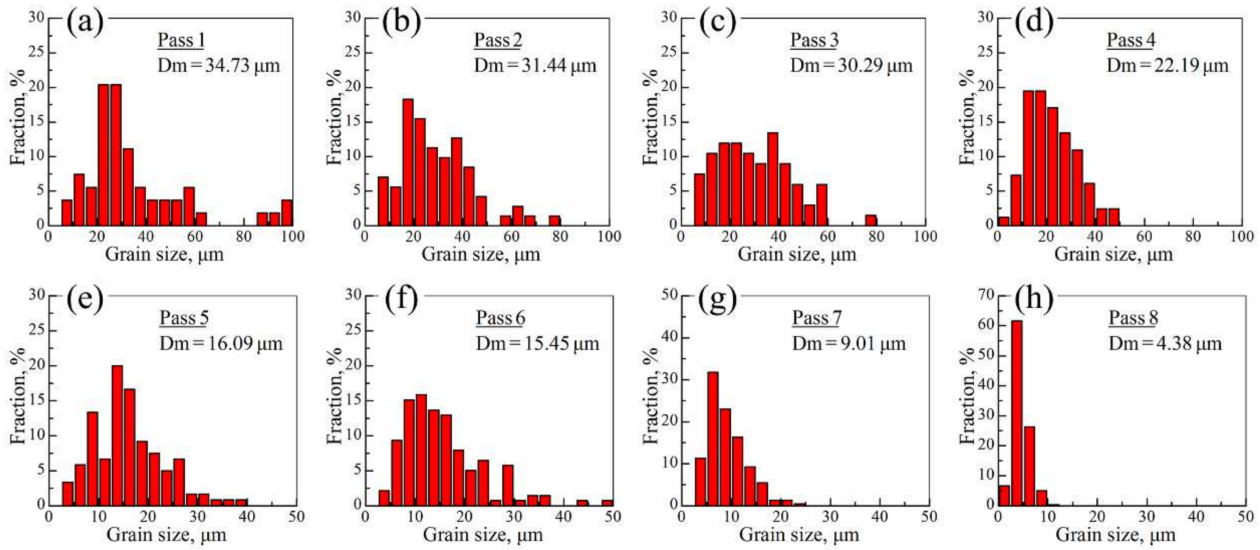

Figure 3. Grain size distributions of AZ31 magnesium alloy sheets during multi-pass lowered-temperature rolling: (**a**) Pass 1; (**b**) Pass 2; (**c**) Pass 3; (**d**) Pass 4; (**e**) Pass 5; (**f**) Pass 6; (**g**) Pass 7; (**h**) Pass 8 (Dm refers to the average grain size).

Further decreasing the rolling deformation increased the degree of DRX, producing a large number of fine, equiaxed grains in the Pass 3 sheet and Pass 4 sheet (Figure 2). Figure 3 shows that their average grain sizes were refined to 30.29 μm in the Pass 3 sheet and 22.19 μm in the Pass 4 sheet. However, from their grain size distributions, 7.27–75.7 μm in the Pass 3 sheet and 3.53–46.21 μm in the Pass 4 sheet, it could be concluded that their microstructure homogeneity was not good enough [19]. Moreover, their coarse grains were highly distorted, suggesting that the new DRX embryo was developing at the grain boundaries [20]. This further demonstrated their mixed microstructure with large and fine grains. After Passes 5 and 6, the abnormally coarse grain had nearly disappeared and the fractions of DRX grain obviously increased (Figure 2e,f). The microstructure homogeneity was distinctly improved compared to the prior microstructure homogeneity, which could be supported by the unimodal grain size distributions (Figure 3e,f). After Pass 7, the microstructure presented a typical DRX microstructure appearance with excellent microstructure homogeneity. The resulting sheet after Pass 8 had the smallest average grain size of 4.38 μm (Figure 3h). The above metallographic results suggested that, based on the principle of multiple DRX, multi-pass lowered-temperature rolling was not only beneficial to refine the grain size but also to improve the microstructure homogeneity. In addition, in order to obtain a better magnesium alloy microstructure in the future, mathematical modeling between the rolling parameters and the DRX grain size should be established based on the Zener–Hollomon law, similar to the mathematical modeling established in the literature [21].

In order to further characterize the DRX behavior during the rolling, the TEM observation and the grain orientation spread (GOS) map was applied for the Pass 8 sheet, as shown in Figure 4. Clearly, Figure 4a shows that each grain interior was clean and uniform. This suggested that no crystal orientation difference occurred in one individual grain and thereby no obvious defects developed in such grains. Additionally, Figure 4b shows the DRX microstructure of the Pass 8 sheet using the GOS map in which the grains were outlined by the high-angle grain boundaries ranging from 15° to 180°, and the grains with the GOS values smaller than 2° were considered to be the DRX grains (blue and green color) according to the literature [22,23]. Obviously, there were only blue- and green-colored grains in the microstructure, again validating the complete DRX behavior in the Pass 8 sheet. These results together demonstrated that the dislocation density was lower due to the complete DRX behavior during the multi-pass lowered-temperature rolling.

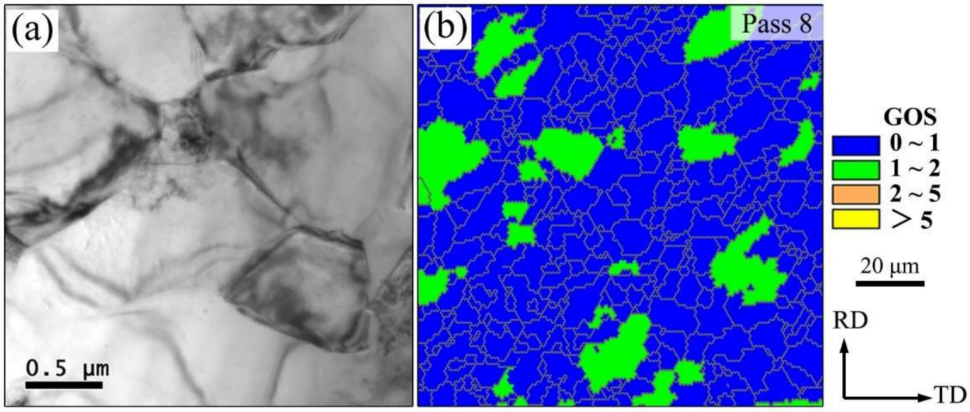

Figure 4. The TEM observations (**a**) and the grain orientation spread (GOS) map for the Pass 8 sheet (**b**). (In GOS map, the GOS value in each grain was determined by calculating the average misorientation between all points within the grain).

3.2. Texture Characteristics

It is well known that the HCP structure in magnesium alloy is liable to cause a strong (0002) basal texture, strongly influencing the mechanical properties [24,25]. Therefore, it was necessary to investigate the texture evolution in multi-pass lowered-temperature rolling. According to the literature [16], the texture state of magnesium alloy can be estimated by both XRD and EBSD. In this work, XRD was applied to measure the texture state of the initial material, and the ratios of the diffraction peaks, I_{10-1}/I_{10-10} and I_{10-11}/I_{0002}, were calculated to quantify the texture characteristics. Figure 5a,b shows the XRD spectrum of the initial material and pure magnesium powder (PDF#35-0821), respectively. Clearly, the ratios of the initial material were similar to those of the standard magnesium card. This suggested that there was no preferred crystalline orientation in the initial material.

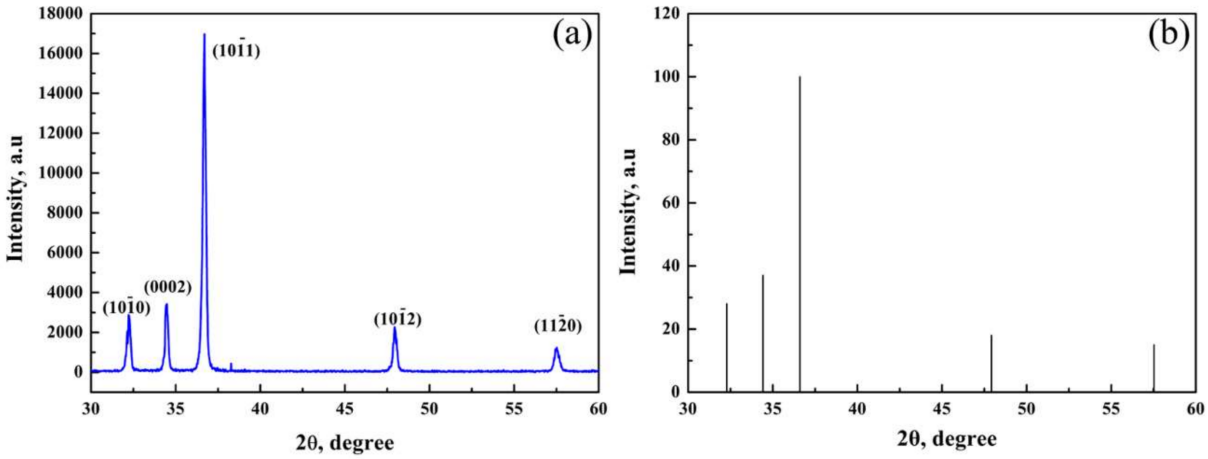

Figure 5. X-ray diffraction spectra of the initial material: (**a**) cast, (**b**) standard spectra.

With regard to the as-rolled sheets, their texture states were measured by EBSD. Figure 6 shows the (0002), (10–10), and (11–20) pole figures under different rolling passes. After one pass, there were multiple peaks in the (0002) pole figures (Figure 6a), and the maximum texture intensity reached 6.01. This demonstrated that the texture morphology emerged in the Pass 1 sheet. After two passes, the peak was not only strengthened but also rotated to the center of the (0002) pole figure (Figure 6b), i.e., more and more c-axes were parallel to the normal direction (ND), and this made the maximum texture intensity increase to 6.5. Wang and Huang pointed out that the stress state under rolling conditions made the slip plane rotate toward the rolling plane and the slip direction toward the

rolling direction [26]. In magnesium alloys, basal slip is the main deformation mode due to its lower critical resolved shear stress (CRSS) [27]. Therefore, the basal plane would gradually rotate to the RD–TD plane under the combined effect of tension along the RD and compression along the ND. However, it can be seen from Figure 6c–e that there were some deflections from the peak to the ND. This could be explained well by the activation of various slip systems. As reported in [28], the CRSS of non-basal slip will decrease sharply when the deformation temperature is higher than 225 °C. In this work, the rolling temperature was always in excess of 260 °C, i.e., non-basal slip (prismatic slip or pyramidal slip) would be activated and take part in the texture formation. According to the above literature [26], these non-basal planes would gradually rotate to the RD–TD plane, and this would rotate the (0002) basal plane away from the RD–TD plane, but due to the tension effect in the RD, the (0002) basal plane only pointed to the RD. Nevertheless, the basal slip was still the dominant deformation mode when the rolling temperature was higher than 260 °C. Such texture evolution could also be characterized by the inverse pole figure (IPF) map, and here the IPF maps for the Pass 4 and Pass 8 sheets were applied, as shown in Figure 7. In these IPF maps, the color code within the unit triangle represented the orientation of the sample normal direction within the hexagonal unit triangle. Clearly, mainly yellow- and red-colored grains were seen in the Pass 4 sheet (Figure 7a). This was consistent with the characteristics in the (0002) pole figure of the Pass 4 sheet (Figure 6c). By comparison, the red-colored grains significantly increased in the Pass 8 sheet, meaning that the texture component whose c-axes were parallel to the ND was strengthened. Therefore, as the rolling proceeded, the overall trend in the (0002) pole figures was still that more and more c-axes pointed to the ND (Figure 6), and the maximum texture intensity gradually increased.

3.3. Mechanical Properties

Figure 8 shows the measured stress–strain curves of the AZ31 magnesium alloy sheets along the RD and the TD in the tension test under different conditions. Table 2 summarizes the corresponding data for the yield stress (YS, MPa), ultimate tensile stress (UTS, MPa), and fracture elongation (FE, %). In order to clearly characterize the evolution of mechanical properties, the variations in YS, UTS, and FE as a function of the rolling pass are displayed in Figure 9. Clearly, the YS and UTS gradually increased with the increase in the rolling pass. As commonly reported [29], the YS of magnesium alloy sheets had a close relationship with the grain size and the texture state. The influence of grain size on the YS followed the Hall–Petch relationship, while the influence of the texture state was based on the Schmid law [29]. Accordingly, the finer grain size and the intense texture state usually led to a higher YS. As previously described, the average grain size retained a refinement trend, while the (0002) basal texture had a strengthening trend. Therefore, in this work, with the increase in the rolling pass, the increasing trend of YS was ascribed to the grain refinement strengthening and the texture strengthening, as shown in Figure 9. In addition, it should be noted that the planar anisotropy in stress (YS and UTS) between the RD and the TD was small (Figure 9 and Table 2). This reason could be ascribed to two points: first, the new DRX grains generally exhibited equiaxed morphology, indicating the similar grain size along any random direction in the sheet; second, owing to the non-texture state in the initial material, the (0002) basal plane would rotate toward the RD–TD plane along any random direction in the sheet, and this led to the small difference in the texture state between the RD and the TD. Therefore, the similar microstructure state was the main reason for the small planar anisotropy between the RD and the TD. In addition, the sheets during the multi-pass lowered-temperature rolling underwent DRX completely, exhibited a lower dislocation density. This made the contribution from the dislocation density to the strength improvement small, which was not considered in this work. Similarly, in AZ31 magnesium alloy, the contribution of solid solution strengthening to the strength was much smaller compared with the fine-grained strengthening, which was estimated in the literature [30]. As a consequence, this work did not discuss the solid solution strengthening.

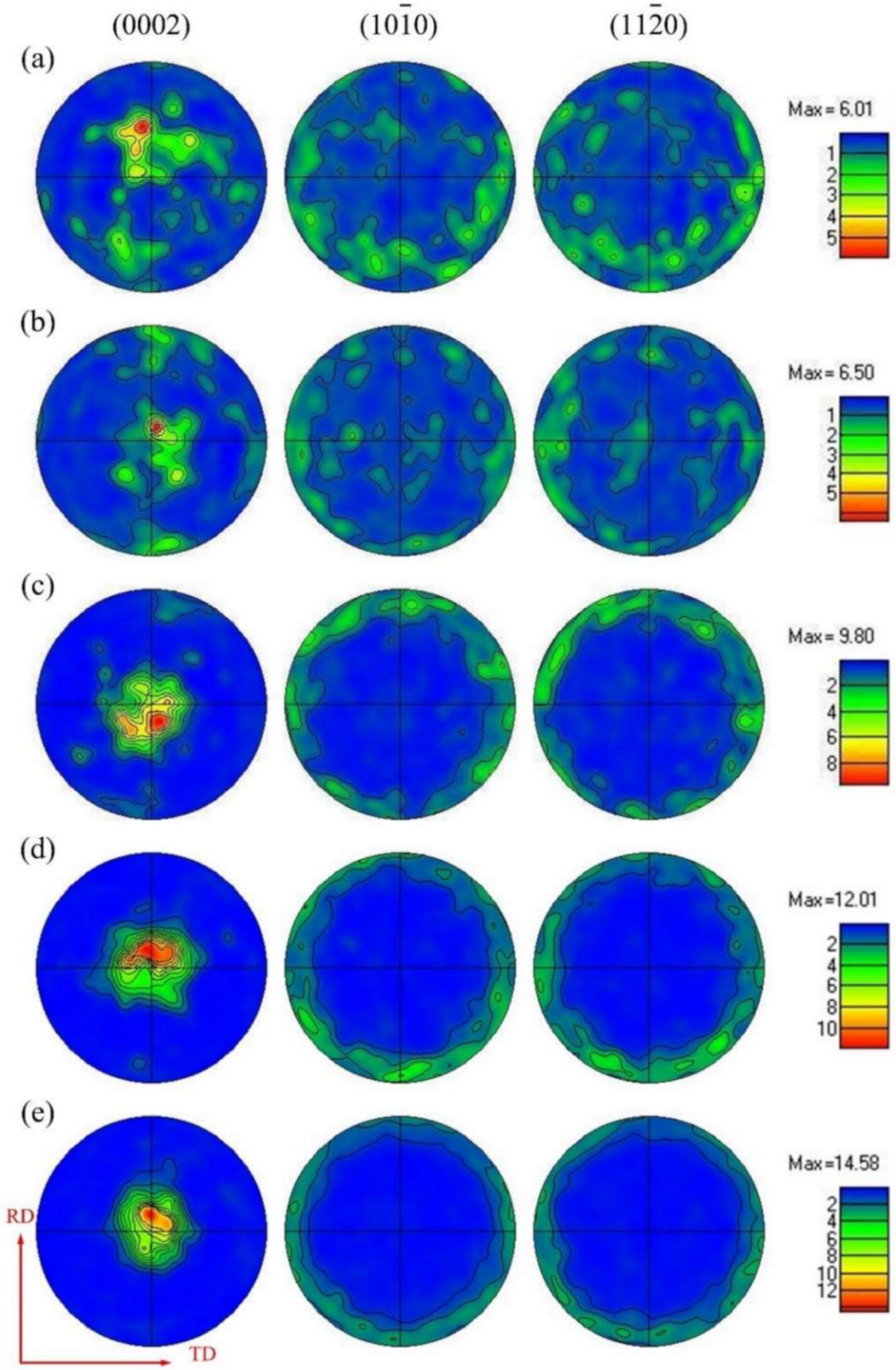

Figure 6. (0002), (10–10), and (11–20) pole figures of AZ31 magnesium alloy sheets during multi-pass lowered-temperature rolling: (**a**) Pass 1; (**b**) Pass 2; (**c**) Pass 4; (**d**) Pass 6; (**e**) Pass 8. (RD: rolling direction, TD: transverse direction).

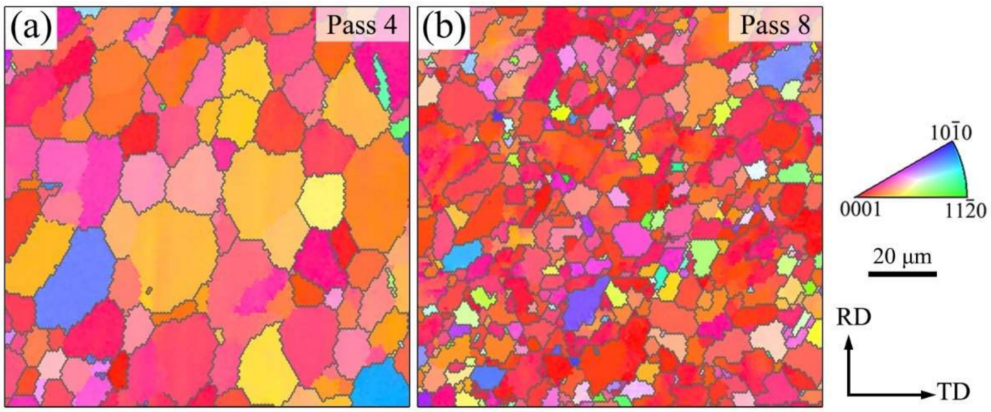

Figure 7. Microstructure characteristics using inverse pole figure maps for the (**a**) Pass 4 sheet and (**b**) Pass 8 sheet.

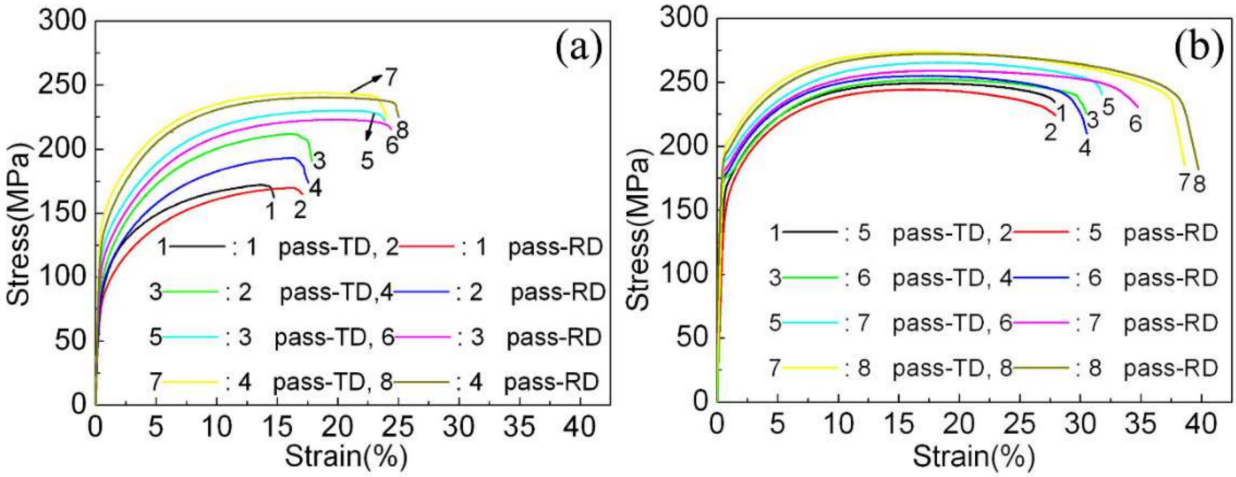

Figure 8. Room temperature stress–strain curves of AZ31 magnesium alloy sheets along the RD and TD during multi-pass lowered-temperature rolling: (**a**) from 1 pass to 4 pass and (**b**) from 5 pass to 8 pass.

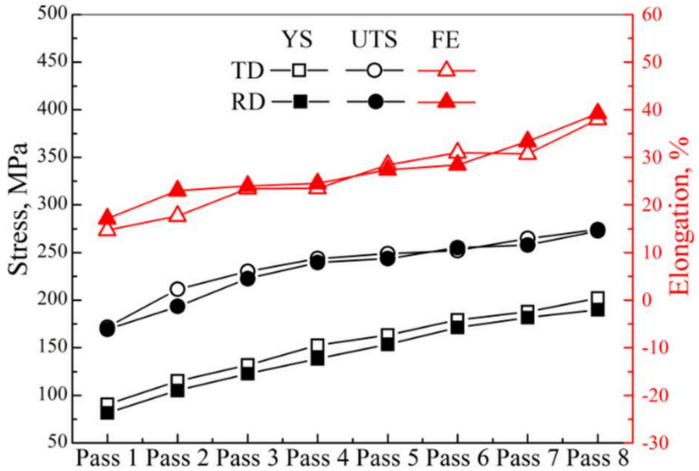

Figure 9. Stress (YS and UTS) and elongation (FE) variation of AZ31 magnesium alloy sheets along the RD and TD during multi-pass lowered-temperature rolling (YS: yield stress; UTS: ultimate tension stress; FE: fracture elongation).

Table 2. Summarized mechanical properties of AZ31 magnesium alloy sheets (YS: yield stress; UTS: ultimate tension stress; FE: fracture elongation).

Condition	YS, MPa		UTS, MPa		FE, %	
	TD	RD	TD	RD	TD	RD
Initial	40		160		7	
Pass 1	90.7	81.6	171.6	169.2	14.7	17.1
Pass 2	115.3	105.2	211.4	193.5	17.7	23
Pass 3	131.9	122.8	230.2	222.6	23.4	24
Pass 4	152.7	138.5	243.5	239.4	23.5	24.5
Pass 5	163.2	153.6	248.9	243.7	28.4	27.4
Pass 6	179.1	171.4	251.8	255.1	31	28.4
Pass 7	188	181.6	264.8	257.9	30.7	33.3
Pass 8	202	189.8	274.3	272.6	38	39.2

For magnesium alloy sheets, poor ductility and formability are the main factors limiting their widespread commercial usability. Therefore, this work focused on the evolution of fracture elongation. Clearly, in both Figure 9 and Table 2, the fracture elongation gradually increased with the increase of the number of rolling passes. The sheets rolled after eight passes exhibited higher fracture elongation (38% along the TD and 39.2% along the RD). To the authors' knowledge, this is not common in previous literature. The main reason was considered to be the finer grain size, which would be carefully discussed from the aspects of metallographic observations, TEM characteristics, and fracture SEM characteristics.

It is well known that a finer grain size has a positive effect on elongation by affecting the contribution of grain boundary sliding [31]. This is supported by Koike, who pointed out that the ability of grain boundary sliding increased with the decline of the grain size, and the contribution to fracture elongation reached 8% when the grain size was less than 8 μm [31]. Many studies also demonstrated that grain boundary sliding was one important factor improving fracture elongation for AZ31 and AZ61 magnesium alloys with grain sizes less than 5 μm [32,33]. Zheng et al. pointed out that the unique combinations of strength and ductility could be realized in bulk polycrystalline pure magnesium by tuning the predominant deformation mode and suggested that the grain boundary sliding governed the plastic deformation in the ultra-fine grain specimen, leading to softening of the material and exceptionally large room temperature tensile elongation up to 65% [34]. In this work, the average grain size of the resulting sheet (Pass 8 sheet) was approximately 4.38 μm, which was conducive to the occurrence of grain boundary sliding. Therefore, grain boundary sliding arising from a finer grain size contributed to the higher fracture elongation of the Pass 8 sheet. In addition, the homogeneous microstructure should be another influential factor. This could be well supported by the metallographic observations of the uniform deformation part and necking part (the part is indicated by the black point in Figure 11a). Clearly, in the uniform deformation part (Figure 10a), most of the grains had equiaxed morphology. For the necking part (Figure 10b), although the grains were elongated along tension deformation, the microstructure was still relatively homogeneous and there was no crack nucleation point. Here, their homogeneous microstructure was beneficial to accommodate the tension deformation between grains and to release the stress concentration around the grain boundaries. This prevented the crack appearing prematurely, which further improved their fracture elongation.

Another mechanism describing the higher fracture elongation of the resulting sheets is the activation of non-basal slips (pyramidal slip or prismatic slip). The activation of non-basal slips would delay the texture strengthening and then release the stress concentration. Koike et al. pointed out that non-basal slips could be activated when the grain size was less than 10 μm, and under this case, the cross-slip of <a> dislocation from the basal to the prismatic plane occurred readily [35]. Similarly, Zhao et al. and Mayama et al. found that the profuse prismatic <a> dislocation activations would suppress twinning formation by rotating grains to preferred orientations for further deformation, resulting

in improved ductility [36,37]. In our recent work, a considerable proportion of prismatic <a> dislocations was activated during the tension deformation of AZ31 magnesium alloys, which was closely related to their higher tensile elongation [38]. The resulting sheet possessed a finer grain size less than 10 μm, which was conducive the activation of non-basal slips. The evidence could be obtained by the TEM characteristics of the necking part of the tension sample (Figure 11). Figure 11a,b depicts abundant dislocation pile-up and twins, respectively. In such a complex dislocation tangle, non-basal dislocations are bound to participate. Therefore, the activation of the non-basal slip produced by a finer grain size partly contributed to the higher fracture elongation.

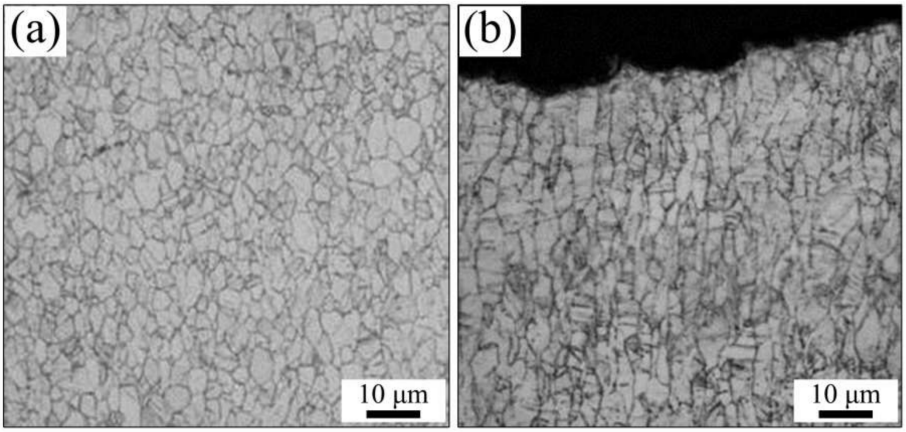

Figure 10. Metallographic observations of the uniform deformation part A (**a**) and necking part B (**b**) indicated by the black point in Figure 11a.

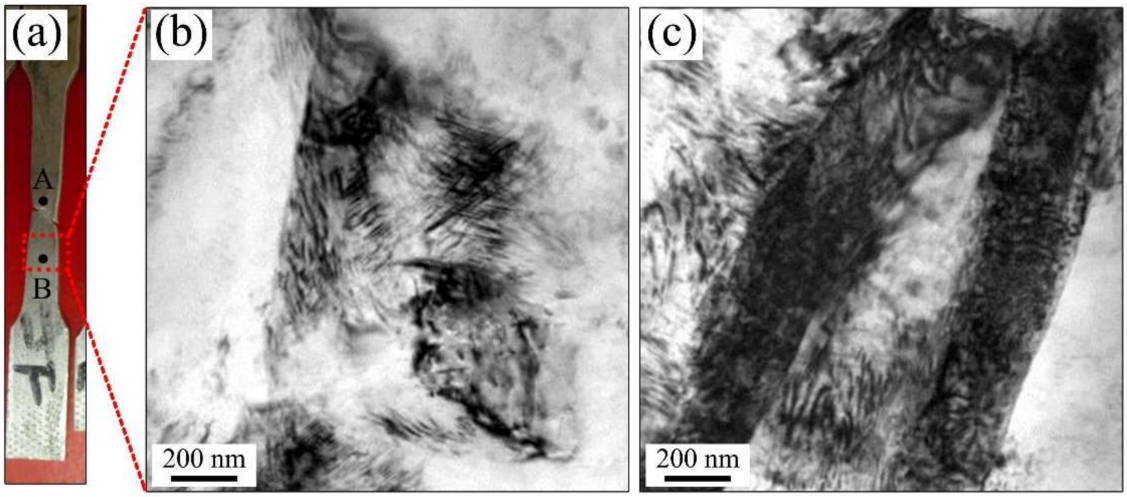

Figure 11. TEM characteristics of the necking part of the AZ31 magnesium alloy sheets after tension deformation: (**a**) tension sample; (**b**) dislocation pile-up; (**c**) twins.

Figure 12 shows the fracture SEM characteristics of the AZ31 tension samples fabricated by multi-pass lowered-temperature rolling. Clearly, the fracture of the as-cast AZ31 tension sample exhibited a typical quasi-cleavage fracture appearance with a smooth cleavage plane and cleavage step (Figure 12a). Similarly, the tension samples after one pass and two passes also had a quasi-cleavage fracture appearance. These features suggested that the above tension samples should undergo brittle failure. However, in Passes 3–5, abundant tear ridges and dimples can be seen in Figure 12d–f. This is generally named the brittle–ductile fracture mode, which is common in magnesium alloy sheets. As the rolling proceeded (a decrease in the grain size), the fracture mode gradually changed from

brittle–ductile fracture to ductile fracture. Finally, because of the smaller grain size (2.5 μm) in the Pass 8 sheet, the tension fracture exhibited typical ductile fracture with dimples.

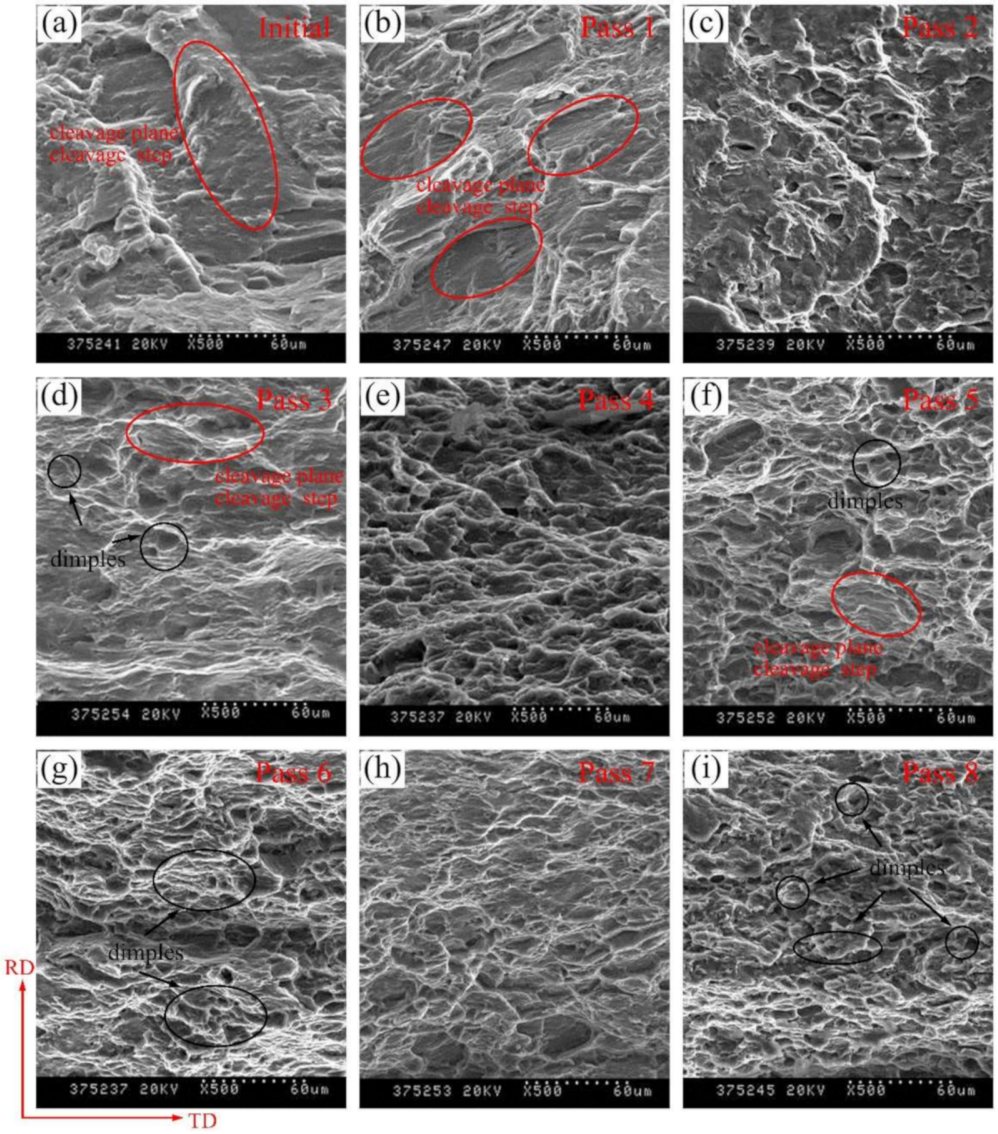

Figure 12. Fracture SEM characteristics of AZ31 tension samples fabricated by multi-pass lowered-temperature rolling: (**a**) Initial; (**b**) Pass 1; (**c**) Pass 2; (**d**) Pass 3; (**e**) Pass 4; (**f**) Pass 5; (**g**) Pass 6; (**h**) Pass 7 and (i) Pass 8.

4. Conclusions

In this work, multi-pass lowered-temperature rolling was applied to fabricate AZ31 magnesium alloy sheets with high mechanical properties. This rolling process not only realized the fabrication of thin sheets but also optimized the microstructure. Due to the effect of multiple dynamic recrystallization, the grain size was obviously refined and the microstructure homogeneity was distinctly improved. The average grain size in the resulting sheet was refined to 4.38 μm. As the rolling proceeded, the (0002) basal plane gradually rotated toward the rolling plane, but the participation of non-basal slip made the (0002) basal plane point slightly toward the RD. These microstructure variations influenced the yield stress greatly. In the resulting sheet, the yield stresses were markedly increased to 202 MPa along the TD and 189.8 MPa along the RD. In addition, the finer grain size was beneficial to the grain boundary sliding and the activation of non-basal slip, which finally improved the fracture elongations. In the resulting sheet, the fracture elongations reached 38% in the TD a nd 39.2% in the RD.

Author Contributions: Conceptualization, W.W. and W.C.; methodology, L.Z., W.W., Z.W., B.S., W.C., Y.Y. and W.Z.; software, Z.W., L.Z., Z.W., B.S., Y.Y. and W.Z.; validation, L.Z., Z.W. and W.C.; formal analysis, B.S. and Y.Y.; investigation, Q.M., W.W. and W.C.; resources, W.C. and W.Z.; data curation, Q.M. and L.Z.; writing—original draft preparation, Q.M.; writing—review and editing, W.W.; visualization, L.Z., Z.W., B.S. and Y.Y.; supervision, B.S., Y.Y. and W.Z.; funding acquisition, W.W., W.C. and W.Z. All authors have read and agreed to the published version of the manuscript.

Funding: This work was funded by the National Natural Science Foundation of China (Grant No. 51975146, 52205344), the Natural Science Foundation of Shandong Province (Grant No. ZR2020QE171, ZR2021ME073), and the Key Research and Development Plan in Shandong Province (Grant No. 2019JZZY010364).

Data Availability Statement: Research data are available upon reasonable request to the authors.

Conflicts of Interest: The authors declare no conflict of interest.

References

1. Zhang, L.; Zhang, J.; Leng, Z.; Liu, S.; Yang, Q.; Wu, R.; Zhang, M. Microstructure and mechanical properties of high-performance Mg-Y-Er-Zn extruded alloy. *Mater. Des.* **2014**, *54*, 256–263. [CrossRef]
2. Da Huo, P.; Li, F.; Wang, Y.; Wu, R.Z.; Gao, R.H.; Zhang, A.X. Annealing coordinates the deformation of shear band to improve the microstructure difference and simultaneously promote the strength-plasticity of composite plate. *Mater. Des.* **2022**, *219*, 110696. [CrossRef]
3. Suh, B.-C.; Shim, M.; Shin, K.S.; Kim, N.J. Current issues in magnesium sheet alloys: Where do we go from here? *Scr. Mater.* **2014**, *84–85*, 1–6. [CrossRef]
4. Chino, Y.; Sassa, K.; Kamiya, A.; Mabuchi, M. Stretch formability at elevated temperature of a cross-rolled AZ31 Mg alloy sheet with different rolling routes. *Mater. Sci. Eng. A* **2008**, *473*, 195–200. [CrossRef]
5. Wang, D.; Liu, S.; Wu, R.; Zhang, S.; Wang, Y.; Wu, H.; Zhang, J.; Hou, L. Synergistically improved damping, elastic modulus and mechanical properties of rolled Mg-8Li-4Y-2Er-2Zn-0.6Zr alloy with twins and longperiod stacking ordered phase. *J. Alloy. Compd.* **2021**, *881*, 160663. [CrossRef]
6. Chen, W.Z.; Yu, Y.; Wang, X.; Wang, E.; Liu, Z. Optimization of rolling temperature for ZK61 alloy sheets via microstructure uniformity analysis. *Mater. Sci. Eng. A* **2013**, *575*, 136–143. [CrossRef]
7. Huang, X.; Chino, Y.; Mabuchi, M.; Matsuda, M. Influences of grain size on mechanical properties and cold formability of Mg–3Al–1Zn alloy sheets with similar weak initial textures. *Mater. Sci. Eng. A* **2014**, *611*, 152–161. [CrossRef]
8. Huang, X.; Suzuki, K.; Chino, Y.; Mabuchi, M. Texture and stretch formability of AZ61 and AM60 magnesium alloy sheets processed by high-temperature rolling. *J. Alloy. Compd.* **2015**, *632*, 94–102. [CrossRef]
9. Huo, Q.; Yang, X.; Sun, H.; Li, B.; Qin, J.; Wang, J.; Ma, J. Enhancement of tensile ductility and stretch formability of AZ31 magnesium alloy sheet processed by cross-wavy bending. *J. Alloy. Compd.* **2013**, *581*, 230–235. [CrossRef]
10. Wang, W.; Chen, W.; Zhang, W.; Cui, G.; Wang, E. Effect of deformation temperature on texture and mechanical properties of ZK60 magnesium alloy sheet rolled by multi-pass lowered-temperature rolling. *Mater. Sci. Eng. A* **2018**, *712*, 608–615. [CrossRef]
11. Cho, J.-H.; Jeong, S.S.; Kang, S.-B. Deep drawing of ZK60 magnesium sheets fabricated using ingot and twin-roll casting methods. *Mater. Des.* **2016**, *110*, 214–224. [CrossRef]
12. Kim, W.; Yoo, S.; Chen, Z.; Jeong, H. Grain size and texture control of Mg–3Al–1Zn alloy sheet using a combination of equal-channel angular rolling and high-speed-ratio differential speed-rolling processes. *Scr. Mater.* **2009**, *60*, 897–900. [CrossRef]
13. Suh, J.; Victoria-Hernández, J.; Letzig, D.; Golle, R.; Volk, W. Enhanced mechanical behavior and reduced mechanical anisotropy of AZ31 Mg alloy sheet processed by ECAP. *Mater. Sci. Eng. A* **2016**, *650*, 523–529. [CrossRef]
14. Zhang, L.; Chen, W.; Zhang, W.; Wang, W.; Wang, E. Microstructure and mechanical properties of thin ZK61 magnesium alloy sheets by extrusion and multi–pass rolling with lowered temperature. *J. Mater. Process. Technol.* **2016**, *237*, 65–74. [CrossRef]
15. Wang, W.; Zhang, W.; Chen, W.; Yang, J.; Zhang, L.; Wang, E. Homogeneity improvement of friction stir welded ZK61 alloy sheets in microstructure and mechanical properties by multi-pass lowered-temperature rolling. *Mater. Sci. Eng. A* **2017**, *703*, 17–26. [CrossRef]
16. Chen, W.Z.; Zhang, W.C.; Zhang, L.X.; Wang, E.D. Property improvements in fine-grained Mg-Zn-Zr alloy sheets produced by temperature-step-down multi-pass rolling. *J. Alloy. Compd.* **2015**, *646*, 195–203. [CrossRef]
17. Prakash, P.; Toscano, D.; Shaha, S.K.; Wells, M.A.; Jahed, H.; Williams, B.W. Effect of temperature on the hot deformation behavior of AZ80 magnesium alloy. *Mater. Sci. Eng. A* **2020**, *794*, 139923. [CrossRef]
18. Zhou, T.; Yang, Z.; Hu, D.; Feng, T.; Yang, M.; Zhai, X. Effect of the final rolling speeds on the stretch formability of AZ31 alloy sheet rolled at a high temperature. *J. Alloy. Compd.* **2015**, *650*, 436–443. [CrossRef]
19. Chen, W.; Wang, X.; Hu, L.; Wang, E. Fabrication of ZK60 magnesium alloy thin sheets with improved ductility by cold rolling and annealing treatment. *Mater. Des.* **2012**, *40*, 319–323. [CrossRef]
20. Young, J.P.; Ayoub, G.; Mansoor, B.; Field, D.P. The effect of hot rolling on the microstructure, texture and mechanical properties of twin roll cast AZ31Mg. *J. Mater. Process. Technol.* **2015**, *216*, 315–327. [CrossRef]

21. Meher, A.; Mahapatra, M.M.; Samal, P.; Vundavilli, P.R.; Shankar, K.V. Statistical Modeling of the Machinability of an In-Situ Synthesized RZ5/TiB_2 Magnesium Matrix Composite in Dry Turning Condition. *Crystals* **2022**, *12*, 1353. [CrossRef]
22. Wang, W.; Cui, G.; Zhang, W.; Chen, W.; Wang, E. Evolution of microstructure, texture and mechanical properties of ZK60 magnesium alloy in a single rolling pass. *Mater. Sci. Eng. A* **2018**, *724*, 486–492. [CrossRef]
23. Imandoust, A.; Barrett, C.D.; Oppedal, A.L.; Whittington, W.R.; Paudel, Y.; El Kadiri, H. Nucleation and preferential growth mechanism of recrystallization texture in high purity binary magnesium-rare earth alloys. *Acta Mater.* **2017**, *138*, 27–41. [CrossRef]
24. Chen, W.Z.; Wang, X.; Kyalo, M.N.; Wang, E.D.; Liu, Z. Yield strength behavior for rolled magnesium alloy sheets with texture variation. *Mater. Sci. Eng. A* **2013**, *580*, 77–82. [CrossRef]
25. Trang, T.T.T.; Zhang, J.H.; Kim, J.H.; Zargaran, A.; Hwang, J.H.; Suh, B.-C.; Kim, N.J. Designing a magnesium alloy with high strength and high formability. *Nat. Commun.* **2018**, *9*, 2522. [CrossRef]
26. Wang, Y.N.; Huang, J.C. Texture analysis in hexagonal materials. *Mater. Chem. Phys.* **2003**, *81*, 11–26. [CrossRef]
27. Li, G.; Zhang, J.; Wu, R.; Feng, Y.; Liu, S.; Wang, X.; Jiao, Y.; Yang, Q.; Meng, J. Development of high mechanical properties and moderate thermal conductivity cast Mg alloy with multiple RE via heat treatment. *J. Mater. Sci. Technol.* **2017**, *34*, 1076–1084. [CrossRef]
28. Wang, W.; Chen, W.; Zhang, W.; Cui, G.; Wang, E. Weakened anisotropy of mechanical properties in rolled ZK60 magnesium alloy sheets with elevated deformation temperature. *J. Mater. Sci. Technol.* **2018**, *34*, 2042–2050. [CrossRef]
29. Liu, D.; Liu, Z.; Wang, E. Effect of rolling reduction on microstructure, texture, mechanical properties and mechanical anisotropy of AZ31 magnesium alloys. *Mater. Sci. Eng. A* **2014**, *612*, 208–213. [CrossRef]
30. Liu, D.; Bian, M.Z.; Zhu, S.; Chen, W.Z.; Liu, Z.; Wang, E.D.; Nie, J. Microstructure and tensile properties of Mg-3Al-1Zn sheets produced by hot-roller-cold-material rolling. *Mater. Sci. Eng. A* **2017**, *706*, 304–310. [CrossRef]
31. Koike, J. Enhanced deformation mechanisms by anisotropic plasticity in polycrystalline Mg alloys at room temperature. *Met. Mater. Trans. A* **2005**, *36*, 1689–1696. [CrossRef]
32. Yoshida, Y.; Arai, K.; Itoh, S.; Kamado, S.; Kojima, Y. Realization of high strength and high ductility for AZ61 magnesium alloy by severe warm working. *Sci. Technol. Adv. Mater.* **2005**, *6*, 185–194. [CrossRef]
33. Koike, J.; Ohyama, R.; Kobayashi, T.; Suzuki, M.; Maruyama, K. Grain-Boundary Sliding in AZ31 Magnesium Alloys at Room Temperature to 523 K. *Mater. Trans.* **2003**, *44*, 445–451. [CrossRef]
34. Zheng, R.; Du, J.-P.; Gao, S.; Somekawa, H.; Ogata, S.; Tsuji, N. Transition of dominant deformation mode in bulk polycrystalline pure Mg by ultra-grain refinement down to sub-micrometer. *Acta Mater.* **2020**, *198*, 35–46. [CrossRef]
35. Koike, J.; Kobayashi, T.; Mukai, T.; Watanabe, H.; Suzuki, M.; Maruyama, K.; Higashi, K. The activity of non-basal slip systems and dynamic recovery at room temperature in fine-grained AZ31B magnesium alloys. *Acta Mater.* **2003**, *51*, 2055–2065. [CrossRef]
36. Zhao, D.; Ma, X.; Srivastava, A.; Turner, G.; Karaman, I.; Xie, K.Y. Significant disparity of non-basal dislocation activities in hot-rolled highly-textured Mg and Mg-3Al-1Zn alloy under tension. *Acta Mater.* **2021**, *207*, 116691. [CrossRef]
37. Mayama, T.; Noda, M.; Chiba, R.; Kuroda, M. Crystal plasticity analysis of texture development in magnesium alloy during extrusion. *Int. J. Plast.* **2011**, *27*, 1916–1935. [CrossRef]
38. Zhang, Z.; Zhang, J.; Wang, W.; Liu, S.; Sun, B.; Xie, J.; Xiao, T. Unveiling the deformation mechanism of highly deformable magnesium alloy with heterogeneous grains. *Scr. Mater.* **2022**, *221*, 114963. [CrossRef]